Backscattered Electron Imaging and Electron Backscattered Diffraction in the Study of Bacterial Attachment to Titanium Alloy Structure

Wang, Anqi; Jones, Ian; Mei, Junfa; Tse, Yau; Landini, Gabriel; Li, Yue; Ke, Linnan; Huang, Yuanli; Liu, Li; Wang, Chunren; Sammons, Rachel

DOI:
10.1111/jmi.12649

Document Version
Peer reviewed version

Citation for published version (Harvard):
Wang, A, Jones, I, Mei, J, Tse, YY, Landini, G, Li, Y, Ke, L, Huang, Y, Liu, L, Wang, C & Sammons, R 2017, 'Backscattered Electron Imaging and Electron Backscattered Diffraction in the Study of Bacterial Attachment to Titanium Alloy Structure', Journal of Microscopy. https://doi.org/10.1111/jmi.12649

Backscattered Electron Imaging and Electron Backscattered Diffraction in the Study of Bacterial Attachment to Titanium Alloy Structure

Journal:	*Journal of Microscopy*
Manuscript ID	JMI-2016-0241.R1
Wiley - Manuscript type:	Original Article
Date Submitted by the Author:	10-Aug-2017
Complete List of Authors:	Wang, Anqi; University of Birmingham, The School of Metallurgy and Materials; China National Institute for Food and Drug Control, Division of Biomaterials and Tissue Engineering Jones, Ian; University of Birmingham, School Metallurgy and Materials Mei, Junfa; University of Birmingham, The School of Metallurgy and Materials Tse, Yau Yau ; University of Birmingham, The School of Metallurgy and Materials Landini, Gabriel; University of Birmingham, Li, Yue; AnEnd Inc. Ke, Linnan; China National Institute for Food and Drug Control, Division of Biomaterials and Tissue Engineering Huang, Yuanli; China National Institute for Food and Drug Control, Division of Biomaterials Liu, Li; China National Institute for Food and Drug Control, Division of Biomaterials Wang, Chunren; China National Institute for Food and Drug Control Sammons, Rachel; University of Birmingham
Keywords:	Electron microscopy, Bacteria adhesion, Grain boundary, Grain orientation, Chemical composition, Microstructure

Backscattered Electron Imaging and Electron Backscattered Diffraction in the Study of Bacterial Attachment to Titanium Alloy Structure

Anqi Wang [a, b, c], Ian P. Jones [a], Gabriel Landini [b], Junfa Mei [a], Yau Y. Tse [a], Yue X. Li [d], Linnan Ke [c], Yuanli Huang [c], Li Liu [c], Chunren Wang [c] and Rachel L. Sammons[b]

a. The School of Metallurgy and Materials, University of Birmingham, Edgbaston, Birmingham, B15 2TT, UK;

b. The School of Dentistry, University of Birmingham, 5 Mill Pool Way, Edgbaston, Birmingham, B5 7EG, UK;

c. Division of Biomaterials and Tissue Engineering, the National Institutes for Food and Drug Control, 31 Huatuo Road, the Biomedicine Industrial Park, Daxing District, Beijing, 102629, China;

d. Axend Inc., 12045E, Waterfront Drive, Suite 450, Los Angeles, California, LA 90094, USA.

Abstract

The application of secondary electron (SE) imaging, backscattered electron imaging (BSE) and electron backscattered diffraction (EBSD) was investigated in this work to study the bacterial adhesion and proliferation on a commercially pure titanium (cp Ti) and a Ti6Al4V alloy (Ti 64) with respect to substrate microstructure

Corresponding author: Rachel Sammons, The School of Dentistry, University of Birmingham, 5 Mill Pool Way, Edgbaston, Birmingham, B5 7EG, UK; Email: r.l.sammons@bham.ac.uk; Phone: +44 (0) 121 466 5542; Fax: 44 (0) 121 466 5501.

and chemical composition. Adherence of Gram-positive *Staphylococcus epidermidis* 11047 and *Streptococcus sanguinis* GW2, and Gram-negative *Serratia* sp. NCIMB 40259 and *Escherichia coli* 10418 was compared on cp Ti, Ti 64, pure aluminium (Al) and vanadium (V). The substrate microstructure and the bacterial distribution on these metals were characterised using SE, BSE and EBSD imaging. It was observed that titanium alloy phase structure, grain boundaries and grain orientation did not influence bacterial adherence or proliferation at micro-scale. Adherence of all four strains was similar on cp Ti and Ti 64 surfaces whilst inhibited on pure Al. This work establishes a non-destructive and straight-forward statistical method to analyse the relationship between microbial distribution and metal alloy structure.

Keywords: Electron microscopy, bacteria adhesion, grain boundary, grain orientation, chemical composition, microstructure.

1 Introduction

Bacterial adhesion, proliferation and the formation of complex biofilms are closely associated with peri-implantitis which is a well known cause of dental implant failures (Costerton *et al.*, 1999). Bacteria adhere onto a biomaterial surface first reversibly but later irreversibly through a series of physical, chemical and molecular interactions (Yuehuei & Richard, 1998). Following adhesion, the bacteria proliferate by growth and division to form colonies which spread and develop into biofilms covering the surface (Katsikogianni & Missirlis, 2004). In the oral cavity this process

can be affected by a number of factors, including the properties of the bacteria themselves, a number of environmental factors including nutritional status, pH, oxygen tension (Bradshaw *et al.*, 1996) and the substrate (Yuehuei & Richard, 1998). Implant surface properties such as wettability, surface roughness and chemical composition are of major significance and have been very well studied (Mabboux *et al.*, 2004, Boulange-Petermann *et al.*, 1993, Vanhaecke *et al.*, 1990, Li & Logan, 2004, Rimondini *et al.*, 2005, Bohinc *et al.*, 2016). The adherence of various bacteria strains was observed to increase with increasing surface roughness on both glass and stainless steel surfaces and was attributed to increased surface area and defects such as cracks, voids and gaps (Bohinc *et al.*, 2016, Bohinc *et al.*, 2014).

Titanium and its alloys are commonly used in a wide range of orthopaedic and dental applications because of their *in vivo* corrosion resistance, excellent mechanical properties and biocompatibility. In the fight against infection it is of great importance to understand how bacterial adhesion, proliferation and biofilm formation are influenced by various titanium surface properties. Recent research in this area has usually focused on the influence of titanium surface roughness, topography and surface modification through means such as ion implantation and antibacterial coatings (Puckett *et al.*, 2010, Park *et al.*, 2008, Yoshinari *et al.*, 2001, Hu *et al.*, 2010). However, surprisingly little is known about the impact of the basic metallurgical features, such as grain boundaries (GB), grain orientations and phase

structure. These features are not only a controllable consequence of the choice of material and the manufacturing methods, but also potential bacterial growth promoters/inhibitors, because of the morphology and energy changes and possible elemental accumulation. Among the limited studies, there is some evidence that bacteria may be sensitive to compositional difference within alloys since *Staphylococcus epidermidis* cells were reported to preferentially attach to the vanadium-rich phase on an etched Ti6 64 alloy (Gabriel *et al.*, 1994) and *Pseudomonas* sp. adhesion to stainless steel was reported to be GB-related (Sreekumari *et al.*, 2001, Sreekumari *et al.*, 2004). More recent work suggests that *Staphylococcus aureus*, *Pseudomonas aeruginosa* and *Escherichia coli* are sensitive to nano-scale crystalline surface since adherence was significantly promoted on an ECAP (equal channel angular pressing)-processed titanium with ultrafine grains (Truong *et al.2009*).

The anti-microbial activity of a prosthetic material such as titanium (and its alloy) in oral prosthetic devices such as dental implant abutments is a major concern. The abutment is usually polished down to Ra<0.2μm to minimise surface features in the hope to limit bacterial attachment and plaque formation and for ease of cleaning (Han *et al.* 2016). Since cp Ti and Ti 64 are the most common materials for dental abutments, it is of clinical importance to understand bacterial behaviour on polished titanium surfaces. Furthermore, if it can be established that bacterial adherence and proliferation is substrate microstructure-related, it might be inhibited simply by

choosing a certain manufacturing method by promoting certain anti-bacteria microstructures such as certain orientations or phase structures and limiting pro-bacteria features like grain boundaries during device manufacturing.

The aim of this study was to determine the effects of GBs and grain orientations of a cp Ti and the phase structure of a Ti 64 alloy on the adhesion of two Gram-positive cocci (*Staphylococcus epidermidis* and *Streptococcus sanguinis*) and two Gram-negative rods (*Escherichia coli* and a species of *Serratia*), and on the proliferation of the Gram-negative *Serratia*. In one study, *Staphylococci* were reported to account for 66% of knee and hip prosthetic joint infections and enterobacteriacea, including *E.coli,* for 17% (Getzlaf *et al,* 2016). Of the staphylococci, *S. epidermidis* is the most frequently isolated coagulase negative staphylococcus from orthopaedic infections (Arciola *et al,* 2005; Ribiero *et al,* 2012).

Oral *Streptococci* are also opportunistic pathogens associated with orthopaedic implant-associated infections (Getzlaf *et al,* 2016). *S.epidermidis* attachment is mediated by attraction between exposed chemical groups in proteins in the bacterial cell wall and the substrate (Getzlaf *et al,* 2016). Subpopulations of some strains of *S.epidermidis*, including NTCT11057, used in this work, possess tufts of fimbriae consisting of accumulation associated protein (Aap), which in a truncated form is associated with biofilm formation (Banner *et al,* 2009). *S. sanguinis* is a primary coloniser which attaches to teeth and other surfaces, including prosthetic devices. Once attached, such bacteria act as bridging organisms, co-aggregating with other

microorganisms to establish the growing biofilm (Okahashi *et al,* 2011). *S. sanguinis* is also found amongst the bacteria in the complex biofilms associated with dental peri-implantitis (Fardal *et al.*, 1999). *S. sanguinis* GW2 are covered with peritrichous filaments of two lengths: fine fibrils approximately 150nm in length and shorter globular fibrils approximately 75nm in length (Handley *et al,* 1985).

In contrast, *Serratia* NCIMB 40259 is a non-pathogenic, non-clinical bacteria which was originally isolated from the soil and has been extensively studied because of its ability to form metal phosphates and potential for environmental remediation. It was selected for this study because it readily forms biofilms on titanium and other surfaces under laboratory conditions. It resembles *E.coli* in possessing cell wall appendages known as curli which are believed to mediate surface attachment (Allan *et al.,* 2002; Macaskie *et al.*, 2005). *E. coli* attachment to abiotic surfaces is mediated by specialised fimbriae known as curli (Getzlaf *et al,* 2016). *Serratia* NCIMB 40259 attachment is also thought to be mediated by curli (Allan *et al,* 2002; Macaskie *et al.*, 2005).

This work is the first to directly visualise bacterial adhesion and proliferation with respect to titanium microstructures at micro-scale to systematically assess their direct impact on bacterial behaviour. It establishes a non-destructive and statistical method to investigate the relationship between microbial distribution and metal

microstructure systematically, based on electron microscopy using secondary/ backscattered electron imaging and electron backscattered diffraction.

2 Materials and methods

2. 1 Metal substrate preparation

Commercially pure titanium (TIMET, UK) and Ti6Al4V (TIMET, UK) discs (Φ:10 mm) were polished to a mirror finish using a series of waterproof silicon carbide papers (Struers, UK), from #400 to #1200, followed by a 9 μm diamond suspension (Struers, UK) and an activated colloidal silica solution (Struers, UK). Polished pure aluminium (Goodfellows, UK) and vanadium discs (kindly provided by Dr Mark Ward, School of Metallurgy and Materials, University of Birmingham), prepared by the same procedure, were used as controls. The specimens were cleaned in acetone, ethanol and distilled water in sequence in an ultrasonic bath.

2. 2 Water contact angle and surface roughness measurement

Water contact angle measurements (WCA) were carried out with distilled water using a custom built contact angle goniometer. Distilled water was applied to the test surface using a 25 μL syringe and the WCA was recorded using a digital video camera and measured using Camtel FTA200 software. Three measurements were taken from each sample and the average value was used.

Substrate surface roughness in terms of Ra, the arithmetic average deviation of the surface valleys and peaks, was measured using a Talysurf 10 kit. Three measurements were taken from each mirror polished sample over a distance of 3 mm.

2. 3 Bacterial adhesion

The bacterial strains used in this study were Gram positive *Staphylococcus epidermidis* NCTC11047 (*S. epidermidis*) and *Streptococcus sanguinis* GW2 (*S. sanguinis*), and Gram-negative *Escherichia coli NCTC*10418 (*E. coli*) and *Serratia* NCIMB 40259 (*Serratia*). The *S.epidermidis* and *E.coli* strains are both standard strains obtained from the National Collection of Type Cultures, Public Health England. *S. sanguinis* strain GW2 was a gift from P. Handley, University of Manchester. It was originally isolated from coronal plaque (Handley *et al.,* 1985). *Serratia* NCIMB 40259 was originally isolated as a species of *Citrobacter* but reclassified as *Serratia* by Pattanapipitpaisal *et al.,* 2002; Macaskie *et al,,* 2005).

The bacteria were grown in tryptone soya broth (TSB, Oxoid) in a shaking incubator overnight and harvested by centrifugation at 3000 rpm at 4 °C for 10 min. *S. epidermidis, E. coli* and *Serratia* were grown aerobically and *S. sanguinis* was cultured in a mixture of 80% N_2, 10% $CO_2$and 10% H_2. The incubation temperature was at 37 °C, or 30 °C for *Serratia*. The cells were washed twice in sterile phosphate buffered saline (PBS) and resuspended in PBS with optical density at 600 nm

wavelength (OD_{600}) adjusted to 0.05. PBS was used as a non-nutrient suspension medium to minimise bacterial proliferation.

To test adhesion, three flasks of bacterial culture were prepared for each strain, and four prepared metal discs, one of each material, were suspended vertically in 200 ml bacterial suspensions in 250 ml- flasks and incubated in the same condition for four hours. It is designed as such so that the solution condition and test environment such as pH and bacterial culture were maintained the same for all four materials during the entire conditioning period.

2. 4 Serratia proliferation

Serratia was cultured in 100 ml carbon-limited minimal medium (Thackray, 2005) in a shaking incubator (150 rpm) at 30 °C for 72 hours. 10 ml of this primary culture were combined with 100 ml minimal medium and cultured for a further 72 hours. This procedure promoted the development of fimbriae which are required for biofilm formation by this bacterium (Thackray, 2005). The metal samples were then suspended vertically in 200 ml of the secondary culture diluted with minimal medium to an OD_{600} of approximately 0.05 and incubated at 30 °C for 24 hours.

2. 5 Sample characterisation

After bacterial adhesion and proliferation, the discs were fixed in 2.5% EM grade glutaraldehyde in 0.1 M sodium cacodylate buffer (pH=7.3) for 10 min and

dehydrated in an ethanol series from 20% to 100% for 10 min in each solution, then critical point dried from liquid CO_2.

2.5.1 Scanning Electron Microscopy

Bacteria on each substrate, in both adhesion and proliferation, were counted using secondary electron (SE) imaging using a field emission gun scanning electron microscope (SEM) (JEOL 7000, Japan). Due to the thinness of the attached bacterial layer, no coating was applied. However, a relatively low accelerating voltage (10 kV) was used to minimise charging and electron beam damage. Ten fields of interest (FOI) were chosen at random from each disc, three discs of each material, and the number of bacteria in each field was recorded. The average numbers of bacteria/FOI were compared on cp Ti, Ti 64, Al and V. The location of adherent bacteria in relation to GBs was determined using direct backscattered electron imaging (BSE) where the bacterium appears as a “dark spot” on the clearly revealed gain structural image. BSE signals are closely related to the chemical composition of the site of interest and therefore is also used to visualise the relation between bacterial distribution and metal alloy phase structure. The substrate chemical composition was studied using energy dispersive X-ray analysis (EDX, Oxford INCA, UK).

2.5.2 Electron Backscatter Diffraction Analysis

Electron backscatter diffraction (EBSD) (Oxford INCA, UK) was used to analyse the

substratum grain orientation of the same FOI as the BSE image. The grain texture was analysed with a misorientation tolerance of 15 degrees. The EBSD and BSE images of the same FOI were superimposed using ImageJ (Rasband, 1997-2011). Euclidean Mapping was used to study the bacterial adhesion in relation to GBs and grain orientation. In both the bacterial adhesion and proliferation experiments, the bacterial layer on the titanium surface was fairly thin, and thus not only almost 'transparent' to the electron beam/signals but also formed no major shield to the microstructure underneath. Nevertheless, 20 kV and a large probe current were used to optimise the EBSD mapping quality.

3 Results

3. 1 Substrate microstructure and chemical composition

The cp Ti used in this study was a single hexagonal closed-packed (hcp) α phase material, with a grain size of 20 to 70 μm; Ti 64 was an α+β two-phase material, with hcp α phase (dark areas) and body-centred cubic (bcc) β phase (bright areas) (Figure 1). EDX analysis showed that the β phase of Ti 64 was richer in V: 14.3±0.4 atomic % compared with 3.6±0.2 atomic % in the α phase.

3. 2 Water contact angle and surface roughness measurements

The WCAs of the substrates are shown in Figure 2. All four were hydrophilic (WCA<90°). Cp Ti and Ti 64 showed similar WCAs (P=0.06), suggesting similar

wettability; cp Ti and Ti 64 were more hydrophilic than Al and V (T test: cp Ti vs Al, P = 0.003; cp Ti vs V, P = 0.005).

Sample discs polished following protocol as described in 2.1 demonstrate similar smooth surfaces with Ra values of 0.04±0.01μm for cp Ti and 0.03±0.02μm for Ti 64. Scanning electron microscopy (Figure 1c) confirms that the sample surfaces for both cp Ti and Ti 64 are smooth without artefacts like grooves or peaks, which assures the influence of surface roughness can be neglected in this work, and surface charge won't be altered due to electron concentration caused by features like grooves and peaks.

3. 3 Bacterial adhesion

SE imaging of bacterial adhesion was shown in Figure 3. The sample was not coated with gold nor carbon as normally done for biological samples as coating will jeopardize GBs and grain orientation examination. As a result, the resolution may suffer due to surface charge of the organic matters.

3.3.1 The influence of GBs and grain orientation

All four types of bacteria were tested but because similar results were obtained with each one, results are only presented for *S. epidermidis*. The distribution of *S. epidermidis* on the substrate is displayed in Figure 4a, with GBs and bacteria highlighted in Figure 4b. In the BSE image shown in Figure 4a, *S. epidermidis* cells

appear as black spots: this is because they are consisted of organic matter with lower atomic number elements than the metal substrates, thus yielding weaker signals. The background in Figure 4a reveals the titanium grain structure: the contrast derived from the grain orientation difference between each individual grain. Clearly, the bacteria adhere randomly, showing no preference for the GBs.

EBSD analysis (Figure 5b) was carried out on the same FOI as Figure 4a to study the relationship between bacterial adhesion and substrate grain orientation with respect to B%/GO% values of each grain orientation (Figure 5c). Here, B% (Equation 1) represents the proportion of bacteria located within an area of specific orientation divided by the total number of bacteria in the FOI, and GO% (Equation 2) represents the area percentage of that orientation.

$$\mathrm{B\%} = \frac{B_x}{B_0} \quad \text{Equation 1}$$

B_x: the number of bacteria located within an area of specific orientation;

B_0: the total number of bacteria in the FOI.

$$\mathrm{GO\%} = \frac{GO_x}{GO_0} \quad \text{Equation 2}$$

GO_x: the total area of a specific orientation;

GO_0: the total area of the FOI.

The B%/GO% value is a direct indication of how the bacterial distribution is related to grain orientation: on grain orientations with B%/GO% higher than 1, bacterial

adhesion is promoted; lower than 1, inhibited; equal to 1, independent. The more significantly B%/GO% diverges from 1, the more prominent is the promotion/inhibition effect of the grain orientation. It can be seen in Figure 5b that most of the error bars overlap and where they do not the results should be interpreted with caution because there were very few bacteria on these orientations. Nevertheless, it can be concluded that the B%/GO% value was around 1 and therefore, *S. epidermidis* showed no preference for any particular grain orientation.

Similar results were obtained from all the other three bacteria, demonstrating that bacterial adhesion on cp Ti was not influenced by the substrate grain orientation.

3.3.2 The influence of surface chemical composition

Ti 64 is the most widely used alloy in orthopaedic and dental implants. The major chemical difference between cp Ti and Ti 64 is the addition of alloying elements Al and V in the latter, which significantly alters not only its chemical composition and microstructure but also the physical properties. For instance The tensile strength of Ti 64 is 895-930 MPa, compared to cp Ti which is only 240-550 MPa (Balazic *et al.*, 2007). To investigate the individual influence of Al and V components on bacterial adherence to the Ti 64 alloy, the four bacterial strains were allowed to adhere to cp Ti, Ti 64, pure Al and pure V. Interestingly, the two Gram-positive and the two Gram-negative bacteria showed opposite patterns of adhesion on cp Ti/ Ti 64 and V which can be seen clearly in Figure 6: whilst the highest numbers of Gram negative strains

(*Serratia* and *E. coli*) were seen on Ti 64 and cp Ti; highest numbers of Gram positive strains (*S. epidermidis* and *S. sanguinis*) were seen on V. All four bacteria adhered as well to cp Ti as they did to Ti 64, with least attachment to Al. The differences were analysed by T-test and P values are shown in Table 1. A significant difference was observed between *Serratia* adhesion on Ti 64 and Al (P=0.0001). The adhesion of *E. coli* on cp Ti and Al, *S. epidermidis* on cp Ti and V, Ti 64 and V also showed significant differences with P values ranging between 0.001 and 0.009.

The relation of bacterial distribution to the phase structure (chemical difference) of Ti 64 was studied using BSE imaging. Due to the small grain size of the substrate used (5~10 μm), which is only a little larger than the length of the *Serratia* and *E. coli* bacteria (2-4 μm), only the distributions of *S. epidermidis* and *S. sanguinis* were examined. The distribution of *S. epidermidis* is shown in Figure 7 and is clearly random. A similar distribution was found with *S. sanguinis*.

3. 4 Bacteria Serratia proliferation

3.4.1 Influence of GBs and grain orientation

Serratia distribution on cp Ti after 24 hours' proliferation is shown in Figure 8. The presence of bacterial colonies along certain GBs as indicated by the arrows in Figure 8 suggests a potential GB-associated proliferation. To test this, a statistical model was built based on image processing (Euclidean Distance Mapping, EDM) and

histogram analysis (Rosenfield & Pfaltz, 1968). EDM was carried out on Figure 9a which shows the GBs present in Figure 8a. The distance of each pixel inside a grain from the nearest GB was recorded in Figure 9b, as was the distance of a bacterium in Figure 8a from the nearest GB in Figure 9c. Histograms of the EDM were then plotted of pixels within each grain (red line) and bacteria (black line) versus distance from GBs in Figure 9d. It is apparent that these two curves follow the same trajectory, indicating that the bacteria do not adhere preferentially to GBs. Otherwise, the bacteria EDM histogram would be localised at the initial part of the graph where the distance away from the GBs is not too.

The influence of grain orientation (Figure 10a) on *Serratia* proliferation (Figure 10b) was analysed as described above and indicates that *Serratia* proliferate equally well regardless of the grain orientation (Figure 10b).

3.4.2 Influence of surface chemical composition

As shown in Figure 11, *Serratia* proliferated slightly better on cp Ti than on Ti 64 although this difference was not significant (P = 0.08); approximately the same numbers of bacteria were seen on V as on Ti 64 (P=0.127) but there were fewer on Al (P=0.007).

4 Discussion

The importance of the microstructure and chemical composition of a material can

never be over-emphasised as these properties determine many of the physical and chemical characteristics of the material and entirely govern its mechanical properties (Hench & Jones, 2005). Nevertheless, only recently did researchers start to investigate bacterial and cellular behaviour in relation to the microstructure and phase structure (chemical composition) of titanium. This study is one of the attempts to investigate the relationship between the titanium metallurgical properties and bacterial growth. Other substrate properties such as surface roughness and surface charge that are known to greatly affect bacterial adhesion are minimised in this study through fine polishing and keeping the solution environment the same for all materials during bacterial attachment and proliferation. This study has established a systematic method which can be used as a statistical approach to analyse the response of bacteria and mammalian cells to the surface microstructure, chemical composition and topography.

4.1 The influence of cp Ti GBs and grain orientations

This study indicates that the GBs of cp Ti itself is not enough either to promote bacterial adhesion (*S. epidermidis*, *S. sanguinis*, *E. coli* and *Serratia*), or to stimulate preferential colonisation (*Serratia*). These phenomena are inconsistent with previous reports of GB-associated bacterial adhesion to stainless steels, which were attributed both to the higher energy at GBs and associated chemical segregation (Sreekumari *et al.*, 2001, Sreekumari *et al.*, 2004). Unlike stainless steels, cp Ti is a

single phase material (EDX quantitative analysis showing 99.81±0.15 atomic% of titanium in the substrate) without significant elemental segregation to the GBs. Therefore, it is possible to investigate the bacterial reaction towards the energy and morphology changes at GBs without the interference of chemical difference. The results of this study lead to the speculation that bacteria are not sensitive the energy change at GBs, and the previously reported GB-associated bacterial attachment may be entirely caused by the chemical difference at the GBs in comparison with areas within each grain. The distance between GBs may, however, be critical since improved bacterial adhesion on a nano-crystalline titanium with much denser GBs has been observed (Truong *et al.*). However instead of being energy-related, the authors attributed it to the increased surface roughness at the nano-scale due to the presence of denser GBs (Truong *et al.*). Sensitivity to nano-scale roughness has also been demonstrated on glass surfaces, not only in terms of increased bacterial number, but also alterations in bacterial morphologies and production of extracellular polymeric substrates, indicating higher cellular metabolic activity on the “nano-rough” surfaces (Mitik-Dineva *et al.*, 2009). Therefore, it can be inferred that bacterial adhesion/colonisation may not be sensitive to the energy and morphology change at single GBs. It is only when elemental segregation occurs (such as stainless steel), or the GBs are so dense that they contribute to the surface roughness (such as nano-crystalline titanium), that bacterial attachment will be promoted.

This study is the first to investigate the relationship between bacterial attachment

and grain orientation. The results indicate no relationship at the microscale-level. However, mammalian cells may be more sensitive since pre-osteoblast responses were reported to be grain orientation-dependent (Faghihi *et al.*, 2006). Osteoblast cell attachment was compared on separate Ti 64 samples with different dominant grain orientation and preferential adhesion was observed on the $(10\bar{1}0)$ orientation dominant surface (Faghihi *et al.*, 2006). This grain orientation-associated mammalian cell adhesion was attributed to a wettability difference on surfaces with different preferential orientations. It is possible that bacteria cannot distinguish the minor difference between different grain orientations of cp Ti at micro-scale and further work with titanium samples with different dominant grain orientations will be used in future investigations.

4.2 The influence of Ti 64 alloying components

The differential adhesion of the two Gram-positive and Gram-negative bacteria to cp Ti, Al and V is interesting and may be attributed to their different cell wall structure and consequent differences in wettability. However, this may vary considerably between different Gram positive and Gram negative bacteria and further work with more bacterial strains under different environmental conditions is necessary to confirm these observations. In spite of the existence of Al and V in Ti 64, all the bacteria tested adhered equally well to both cp Ti and Ti 64: This comparable adhesion between the two titanium systems is in good accordance with various

previous reports, and is attributed to the similar surface wettability of the two substrates (Mabboux *et al.*, 2004, Gabriel *et al.*, 1994).

Aluminium was found to inhibit both bacterial adhesion and growth in this study. This has not previously been reported although Illmer and Schinner reported that motility of *Pseudomonas* sp. and *Arthrobacter* sp. was decreased by Al^{3+} (Illmer & Schinner, 1997).

The surface chemical composition of titanium appears to have a major influence on bacterial adhesion and potentially on the subsequent biofilm formation. An *in vivo* study of early clinical plaque formation on dental implants has indicated that incorporated ions such as fluoride and chloride promote plaque formation (Rimondini *et al.*, 2003). However, investigations of the influence of chemical differences are usually limited to coated or chemically modified surfaces, whilst the relationship between bacterial attachment and the phase structure of alloy surface is poorly understood. However Gabriel *et al.* reported that *Staphylococcus epidermidis* (RP12) preferentially attached to the V-rich zone on a Ti 64 alloy (Gabriel *et al.* 1994). This was not seen with *S. epidermidis* and *S. sanguinis* in this study possibly because the Ti 64 substrate used in their work was etched before being exposed to the bacterial cell suspension and the bacteria responded to etching-induced roughness rather than the surface chemistry difference. To avoid such confusion, smooth polished surfaces were used in this study. Contrary to their observation, selective colonisation

was not observed with *S. epidermidis* and *S. sanguinis*. (S*erratia* and *E. coli* bacteria have a similar size to the grains in the Ti 64 used in this study. Their distribution in relation to the Ti 64 phase structure could not be analysed, although it would be possible with materials of larger grain size.) Although surface chemical composition may influence bacterial adhesion, as indicated by the differential adhesion on cp Ti, pure Al and pure V shown in Figure 6, the slight difference between the two phases in Ti 64 is not sufficient to influence the bacterial behaviour.

After proliferation for 24 hours, the number of *Serratia* was slightly higher on cp Ti than on Ti 64 although this difference was not significant. Both the adhesion and proliferation of *Serratia* were significantly lower on Al when compared to the other three metals, suggesting the role of Al as potential bacterial growth inhibitor. It is possible that a gradual breakdown of the protective oxide layer on Ti 64 allows Al to be exposed to the bacteria, leading to the inhibited bacterial growth on Ti 64. This has potential clinical significance and merits further investigation.

5 Conclusions

The results of this study suggest that under the experimental conditions tested:

Bacterial adhesion and proliferation are independent of the GBs and grain orientations of cp Ti. Similar numbers of bacteria attach to cp Ti and Ti 64 which have equal surface wettability but different microstructure and chemical composition.

The experiments suggest that Gram-positive and negative bacteria have different affinities for cp Ti, Ti 64, Al and V, and Al inhibits bacterial adhesion and proliferation both in the pure state and when incorporated into alloy. Further work is necessary to determine whether this could be exploited to combat infection.

6 Acknowledgements

The water contact angle measurements in this study were carried out by Mr Chun Ling Yeung and Prof Jon Preece in the School of Chemistry, University of Birmingham. We thank Prof Lynne Macaskie and Dr Ping Yong in the School of Bioscience, University of Birmingham, for sharing their knowledge of *Serratia*. AW is grateful to the University of Birmingham for an Overseas Research PhD studentship. AW also thanks the State key project (project number: 2016YFC1103201).

Reference

Arciola, C. R., Campoccia, D., Gamberini, S., Donati, M. E., Pirini, V., Visai, L., Speziale, P. & Montanaro, L. (2005) Antibiotic resistance in exopolysaccharide-forming Staphylococcus epidermidis clinical isolates from orthopaedic implant infections. *Biomaterials,* **26,** 6530-6535.

Balazic, M., Kopac, J., Jackson, M. J. & Ahmed, W. (2007) Review: titanium and titanium alloy applications in medicine. *International Journal of Nano and Biomaterials,* **1,** 3-34.

Boulange-Petermann, L., Baroux, B. & Bellon-Fontaine, M.-N. (1993) The influence of metallic surface wettability on bacterial adhesion. *Journal of Adhesion Science and Technology,* **7,** 221-230.

Bradshaw, D. J., Marsh, P. D., Allison, C. & Schilling, K. M. (1996) Effect of Oxygen, Inoculum Composition and Flow Rate on Development of Mixed-Culture Oral Biofilms. *Microbiology,* **142,** 623-629.

Costerton, J. W., Stewart, P. S. & Greenberg, E. P. (1999) Bacterial biofilms: acommon cause of persistent infections. *Science,* **284,** 1318-1322.

Faghihi, S., Azari, F., Li, H., Bateni, M. R., Szpunar, J. A., Vali, H. & Tabrizian, M. (2006) The significance of crystallographic texture of titanium alloy substrates on pre-osteoblast responses. *Biomaterials,* **27,** 3532-3539.

Fardal, Ø., Johannessen, A. C. & Olsen, I. (1999) Severe, rapidly progressing peri-implantitis. *Journal of Clinical Periodontology,* **26,** 313-317.

Banner, M., Cunniffe, J., Macintosh, R., Foster, T., Rohde, H., Mack, D., Hoyes, E., Derrick, J., Upton, M. and Handley, P. (2007) Localized Tufts of Fibrils on *Sraphylocossus epidermidis* NCTC 11047 Are Comprised of the Accumulation-Associated Protein. *Journal of Bacteriology*, **189,** 2793-2804.

Gabriel, B. L., Gold, J., Gristina, A. G., Kasemo, B., Lausmaa, J., Harrer, C. & Myrvik, Q. N. (1994) Site-specific adhesion of *Staphylococcus epidermidis* (RP12) in Ti-Al-V metal systems. *Biomaterials,* **15,** 628-634.

Hench, L. & Jones, J. (2005) *Biomaterials, artificial organs and tissue engineering,* Woodhead publishing Limited, Cambridge.

Hu, X., Neoh, K.-G., Shi, Z., Kang, E.-T., Poh, C. & Wang, W. (2010) An in vitro assessment of titanium functionalized with polysaccharides conjugated with vascular endothelial growth factor for enhanced osseointegration and inhibition of bacterial adhesion. *Biomaterials,* **31,** 8854-8863.

Illmer, P. & Schinner, F. (1997) Influence of aluminum on motility and swarming of *Pseudomonas* sp. and *Arthrobacter* sp. *FEMS Microbiology Letters,* **155,** 121-124.

Katsikogianni, M. & Missirlis, Y. F. (2004) Concise review of mechanisms of bacterial adhesion to biomaterials and of techniques used in estimating bacterial-material interactions. *European Cells and Materials,* **8,** 37-57.

Li, B. & Logan, B. E. (2004) Bacterial adhesion to glass and metal-oxide surfaces. *Colloids and Surfaces B: Biointerfaces,* **36,** 81-90.

Mabboux, F., Ponsonnet, L., Morrier, J.-J., Jaffrezic, N. & Barsotti, O. (2004) Surface free energy and bacterial retention to saliva-coated dental implant materials -- an *in vitro* study. *Colloids and Surfaces B: Biointerfaces,* **39,** 199-205.

Macaskie, L. E., Yong, P., Paterson-Beedle, M., Thackray, A. C., Marquis, P. M., Sammons, R. L., Nott, K. P. & Hall, L. D. (2005) A novel non line-of-sight method for coating hydroxyapatite onto the surfaces of support materials by biomineralization. *Journal of Biotechnology,* **118,** 187-200.

Mitik-Dineva, N., Wang, J., Truong, V., Stoddart, P., Malherbe, F., Crawford, R. & Ivanova, E. (2009) *Escherichia coli*, *Pseudomonas aeruginosa*, and *Staphylococcus aureus* attachment patterns on glass surfaces with nanoscale roughness. *Current Microbiology,* **58,** 268-273.

Park, M. R., Banks, M. K., Applegate, B. & Webster, T. J. (2008) Influence of nanophase titania topography on bacterial attachment and metabolism. *International Journal of Nanomedicine,* **3,** 497-504.

Puckett, S. D., Taylor, E., Raimondo, T. & Webster, T. J. (2010) The relationship between the nanostructure of titanium surfaces and bacterial attachment. *Biomaterials,* **31,** 706-713.

Rasband, W. S. (1997-2011) ImageJ. National Institutes of Health, Bethesda, Maryland, USA.

Rimondini, L., Fare, S., Chiesa, R., Pedeferri, M. P. & Carrassi, A. (2003) The effect of composition, wettability and roughness of the substrate on in vivo early bacterial colonization of titanium. *Journal of Applied Biomaterials and Biomechanics,* **1,** 131-138.

Rimondini, L., Fini, M. & Giardino, R. (2005) The microbial infection of biomaterials: a challenge for clinicials and researchers. A short review. *Journal of Applied Biomaterials and Biomechanics,* **3,** 1-10.

Rosenfield, A. & Pfaltz, J. L. (1968) Distance Functions in Digital Pictures. *Pattern Recognition,* **1,** 33-61S.

Sreekumari, K., Nandakumar, K. & Kikuchi, Y. (2001) Bacterial attachment to stainless steel welds: significance of substratum microstructure. *Biofouling,* **17,** 303-316.

Sreekumari, K., Takao, K., Ujiro, T. & Kikuchi, Y. (2004) High nitrogen stainless steel as a preferred substratum for bacteria and other microfouling organisms *ISIJ International* **44,** 858-864.

Thackray, A. C. (2005) Bacterial biosynthesis of a bone substitute material. In: *School of Dentistry.* University of Birmingham, Birmingham.

Truong, V. K., Lapovok, R., Estrin, Y. S., Rundell, S., Wang, J. Y., Fluke, C. J., Crawford, R. J. & Ivanova, E. P. (2009) The influence of nano-scale surface roughness on bacterial adhesion to ultrafine-grained titanium. *Biomaterials,* **31,** 3674-3683.

Vanhaecke, E., Remon, J., Moores, M., Raes, F., Rudder, D. & Peteghem, A. (1990) Kinetics of *Pseudomonas aeruginosa* adhesion to 304 and 316-L stainless steel: role of cell surface hydrophobicity. *Applied and Environmental Microbiology,* **56,** 788-795.

Yoshinari, M., Oda, Y., Kato, T. & Okuda, K. (2001) Influence of surface modifications to titanium on antibacterial activity in vitro. *Biomaterials,* **22,** 2043-2048.

Yuehuei, H. A. & Richard, J. F. (1998) Concise review of mechanisms of bacterial adhesion to biomaterial surfaces. *Journal of Biomedical Materials Research,* **43,** 338-348.

Bohinc, K., Dražić, G., Abram, A., Jevšnika, M., Jeršek, B,. Nipič, D., Kurinčič, M. & Raspor, P. (2016) Metal surface characteristics dictate bacterial adhesion capacity. *International Journal of Adhesion and Adhesives*, **68,** 39-46.

Bohinc, K., Dražić, G., Fink. R., Oder. M., Jevšnika, M., Nipič, D., Godič-Torkar, K., & Raspor, P. (2014) Available surface dictates microbial adhesion capacity. *International Journal of Adhesion and Adhesives,* **50,** 265-272.

Okahashi, N., Nakata, M., Terao, Y., Isoda, R., Sakurai, A., Sumitomo, T., Yamaguchi, M., Kimura, R., Oiki, E., Kawabata, S & Ooshima, T. (2011) Pili of oral *Streptococcus sanguinis* bind to salivary amylase and promote the biofilm formation. *Microbial pathogenesis*, **50**, 148-154.

Han, A., Tsoi, J., Rodrigues, F., Leprince, J. & Palin, W. (2016) Bacterial adhesion mechanisms on dental implant surface and the influencing factors. *International Journal of Adhesion and Adhesives,* **69,** 58-71.

Handley, P., Carter, P., Wyatt, J. & Hesketh, L. (1985) Surface Structures (Peritrichous Fibrils and Tufts of Fibrils) Found on *Streptococcus sanguis* Strain May be Related to Their Ability to Coaggerate with Oral Genera. *Infection and Immunity*, **47**, 217-227.

Pattanapipitpaisal, P., Mabbet, A., Finlay, J., Beswick, A., Paterson-Beedle, M., Essa, A., Wright, J., Tolley, M., Badar, U., Ahmed, N., Hobman, J., Bron, N. & Macaskie, L. (2002) Reduction of Cr (VI) and bioaccumulation of chromium by Gram positive and Gram negatice microorganisms not previously exposed to Cr-stress.*Environmental Technology*, **23**, 731-745.

Getzlaf, M., Lewallen, E., Kremers, H., Jones, D., Bonin, C., Dudakovic, A., Thaler, R., Cohen, R., Lewallen, D. and Wijnen, A. (2016) Multi-disciplinary antimicrobial strategies for improving orthopaedic implants to prevent prosthetic joint infections in hip and knees. *Journal of Orthopaedic Research,* **34**, 177-186.

Ribeiro, M., Monteiro, F. and Ferraz, M. (2012) Infection of orthopedic implants with emphasis on bacterial adhesion process and techniques used in studying bacterial-material interactions. *Biomatter*, **2**, 176-194.

Allan, V., Callow, M., Macaskie, L. and Paterson-Beedle, M. (2002) Effect of nutrient limitation on biofilm formation and phsphatase activity of a *Citrobacter* sp.. *Microbiology*, **148**, 277-288.

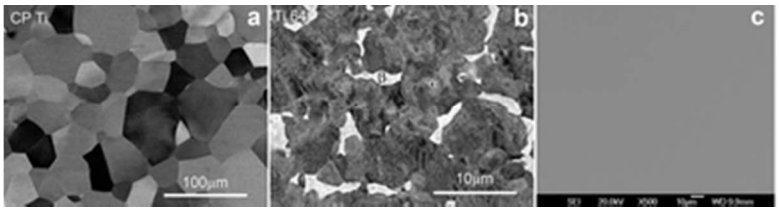

Figure 1 The microstructure of cp Ti (a) and Ti 64 (b) (BSE imaging) and a representative topography of polished cp Ti (c) (SE imaging). The topography of polished Ti64 is similar as shown in (c). α: hcp-phase. β: bcc-phase.

33x8mm (300 x 300 DPI)

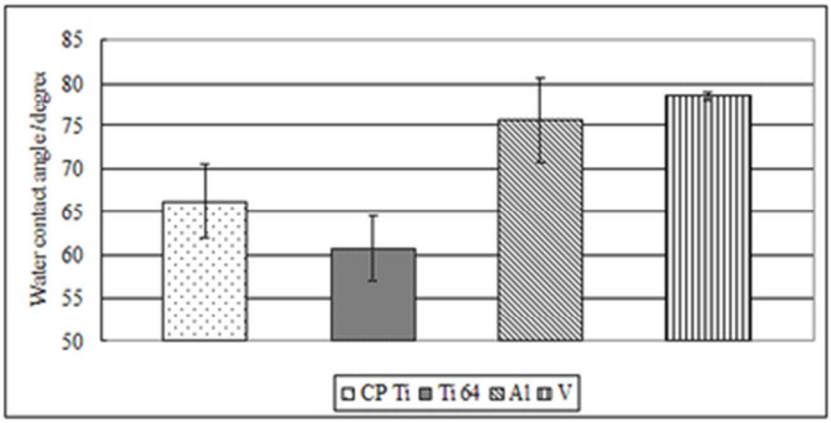

Figure 2 Water contact angle measurements of cp Ti, Ti 64, Al and V.

35x17mm (300 x 300 DPI)

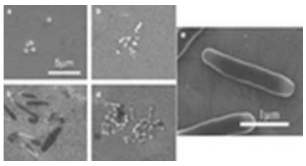

Figure 3 The morphology of S. epidermidis on CP Ti (a), S. sanguinis on CP Ti (b), Serratia on CP Ti (c) and E. coli on Ti 64 (d). (The scale bar in (a) applies to (b) and (c).) (e) shows the morphology of Serratia at higher magnification on Ti 64 showing suspected fimbriae spreading around the bacterium.

6x3mm (600 x 600 DPI)

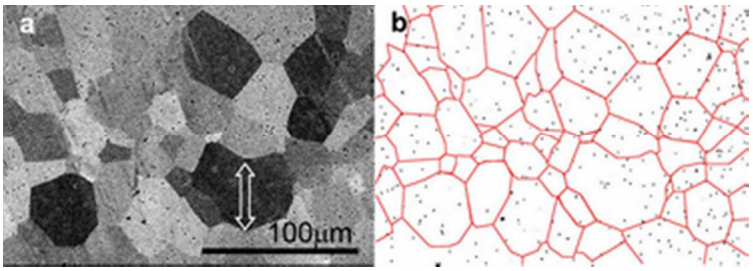

Figure 4 The relationship of S. epidermidis adhesion to cp Ti GBs.
a: The distribution of S. epidermidis on cp Ti (BSE imaging). The black spots are the cells and the background demonstrates the titanium grain structure.
b: Processed image of (a) with only the bacteria (black) and the GBs (red) highlighted (image processed using Photoshop).

31x11mm (300 x 300 DPI)

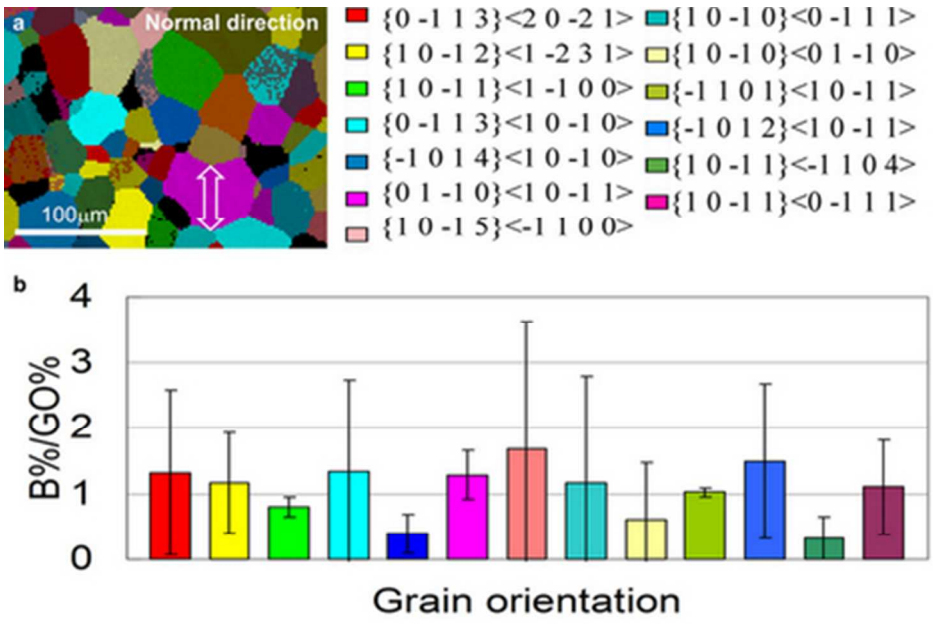

Figure 5 The relationship of S. epidermidis adhesion to cp Ti grain orientation.
a: EBSD texture map of the FOI in Figure 4a with 15° spread (normal direction). A same grain is labelled by a double-headed arrow in both Figure 4a and Figure 5a. Each grain orientation is represented by a different colour, as indexed to the right of the image.
b: Statistic analysis of bacterial distribution in relation to substratum grain orientation. B%: the percentage of bacteria in the area of the same texture; GO%: the area covered by the corresponding texture.

40x26mm (300 x 300 DPI)

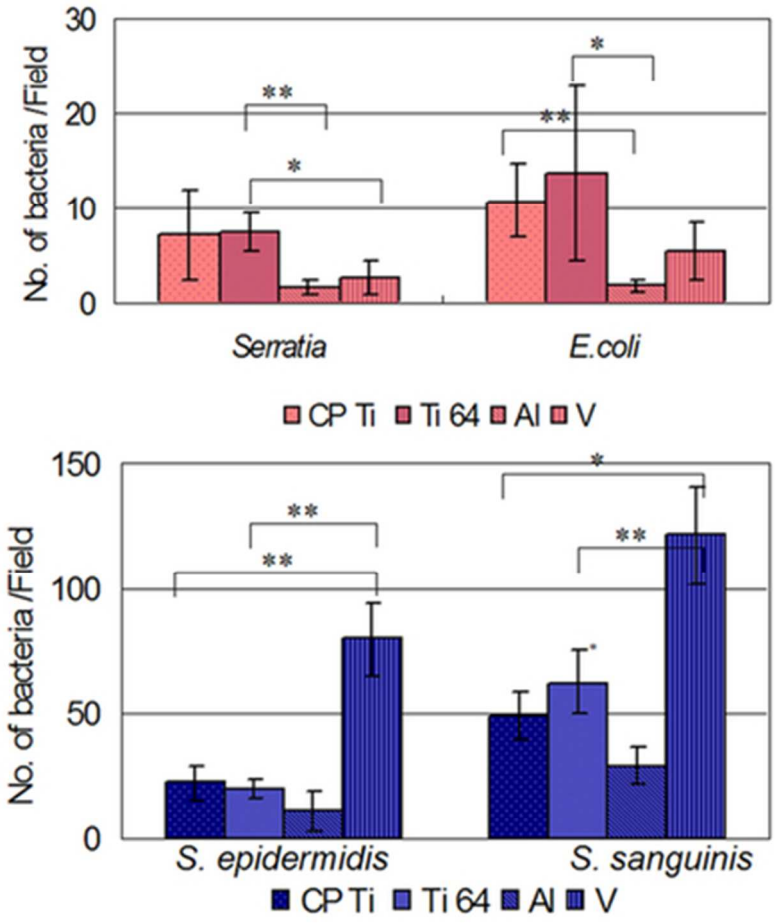

Figure 6 Adhesion of Serratia and E. coli (Gram negative), S. epidermidis and S. sanguinis (Gram positive) to cp Ti, Ti 64, Al and V, respectively.

35x41mm (300 x 300 DPI)

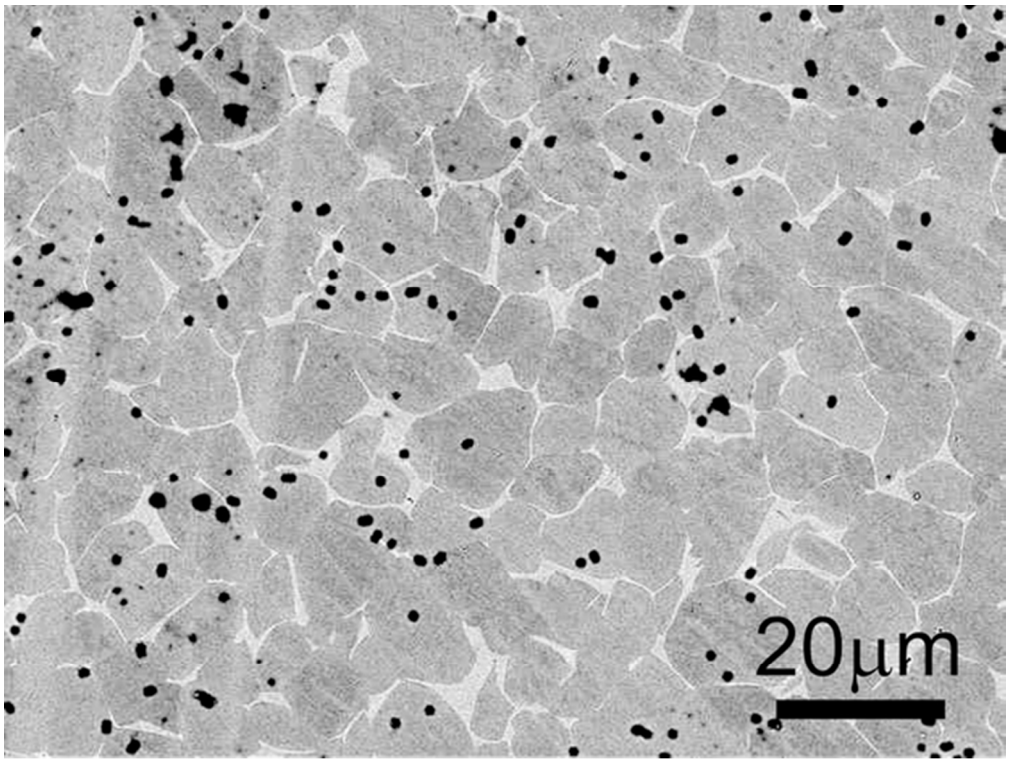

Figure 7 The relationship of S. epidermidis adhesion (black spot) to Ti 64 two-phase structure (background) (BSE imaging).

52x39mm (300 x 300 DPI)

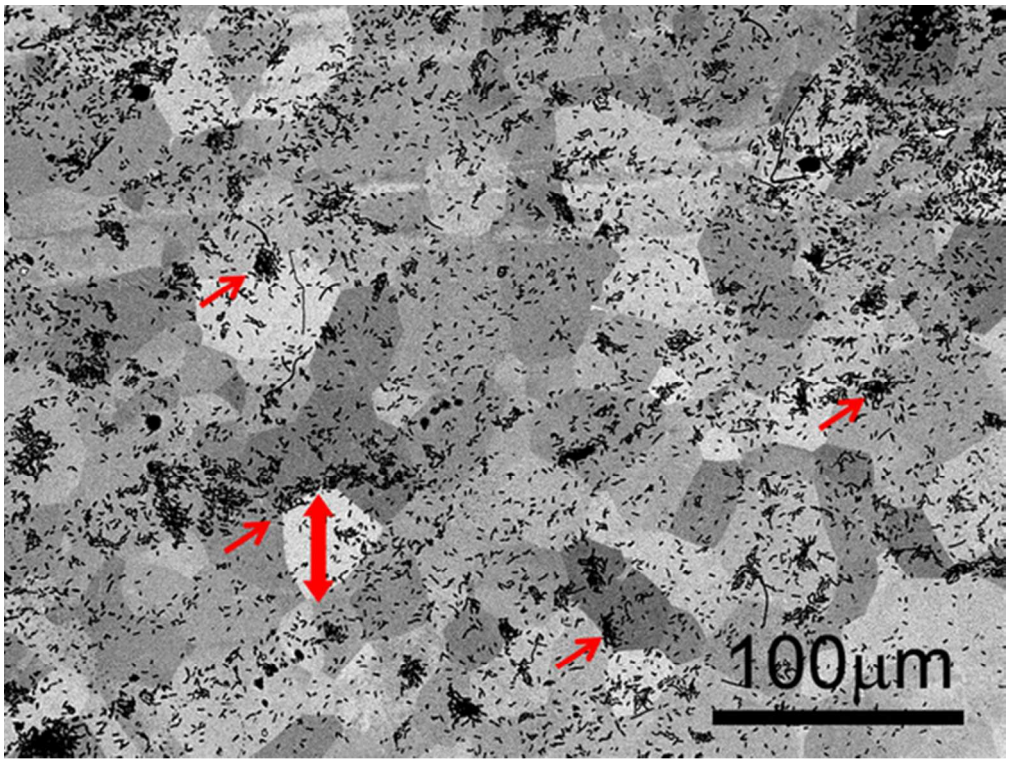

Figure 8 Serratia proliferation on cp Ti (BSE image). The image background illustrates the cp Ti grain structure, whist the locations of bacteria (colonies) are indicated by the black spots/clumps. The single headed arrows points to bacterial colonies adjacent to substrate GBs.

49x37mm (300 x 300 DPI)

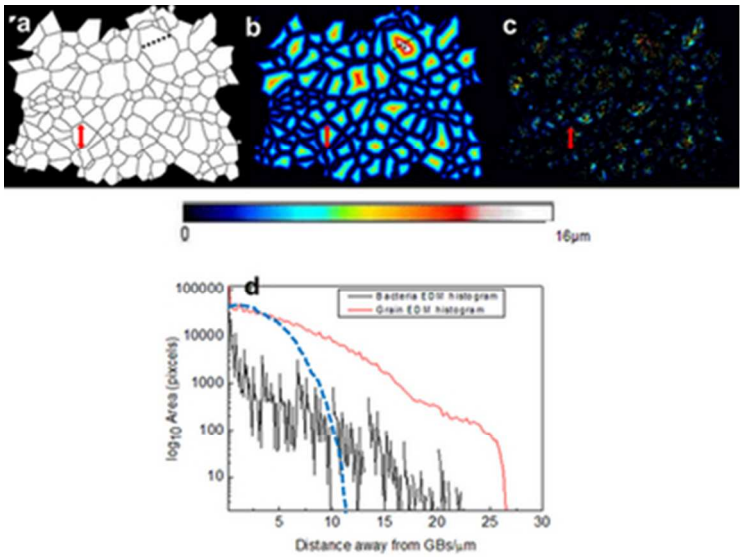

Figure 9 Quantification of Serratia proliferation with respect to cp Ti grain boundaries.
a: GBs in Figure 8 were highlighted. (GBs that touch the image frame were trimmed to avoid incomplete grain size computation.)
b: The points inside each grain were labelled with their distances away from the nearest GBs (Grain EDM). The distance was presented by the colour scale bar below. For example, the black lines will be GBs as their distance is 0 (excluding the image borders). The points marked by "*" in (b) is approximately 16 μm away from the GB, which makes the grain around 50 μm wide along the dotted line, with reference to the red dotted line in Figure 8.
c: The bacteria in Figure 8 were labelled with the value of their distances to the GBs by computing the logical "AND" operation between the bacterial profiles and the Euclidean distance transform of the grain areas. A subsequent histogram of the result provides a function of bacterial presence as a function of the distance to the GBs (Bacteria EDM). The double-headed arrows marked (the location of) the same grain in Figure 8 and Figure 9a-c.
d: Histogram of (b) and (c). If bacterial distribution was strongly associated with GB, the bacterial EDM curve should follow the blue dotted line which reflects the situation when most of the bacteria present near GBs. How strongly the curve is shifted toward the origin will depend on both the size of the bacteria and the size of the cell colonies.

31x24mm (300 x 300 DPI)

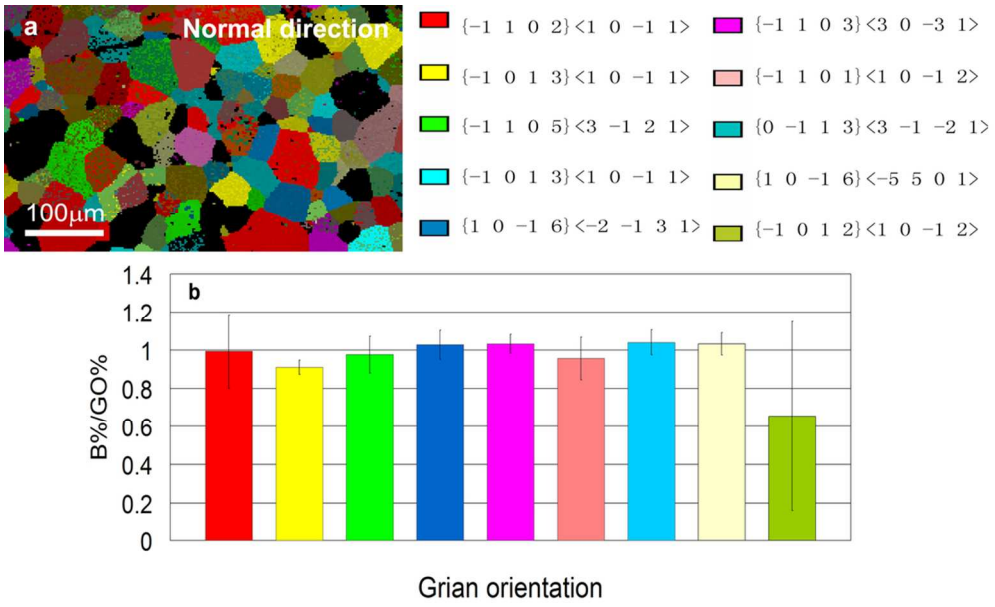

Figure 10 The relationship of Serratia proliferation to cp Ti grain orientation.
a: EBSD map of the FOI in Figure 8 showing the substrate grain texture (with 15° spread).
b: Statistic analysis of bacterial distribution in relation to substratum grain orientation. B%: the percentage of the bacteria on the same grain orientation; GO%: area coverage contributed by the corresponding texture. The colour of each column represents the orientation component shown in (a).

101x63mm (300 x 300 DPI)

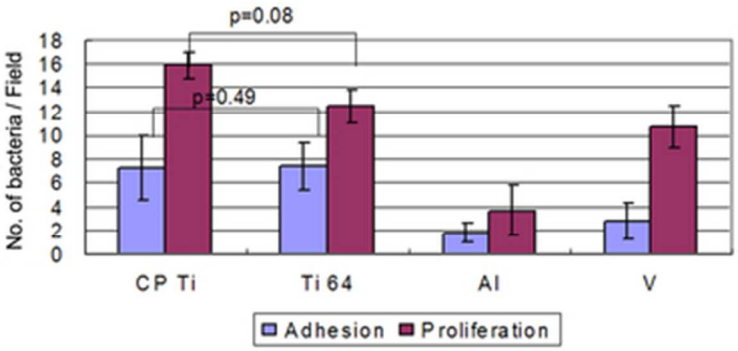

Figure 11 Comparison of adherence and proliferation of Serratia on cp Ti, Ti 64, Al and V.

32x15mm (300 x 300 DPI)

Lay Description

The application of scanning electron microscopy and its various modes was investigated in this work to study the bacterial adhesion and proliferation on polished pure titanium and its alloy (Ti6Al4V) to investigate the influence of substrate microstructure and chemical composition. Adherence of two Gram-positive bacterial strains, and two Gram-negative ones was compared and the bacterial distribution with respects to substrate microstructure quantified. It was observed that titanium alloy phase structure, grain boundaries and grain orientation did not influence bacterial adherence or proliferation at micro-scale. Adherence of all four strains was similar on the two titanium surfaces whilst inhibited on pure aluminium. This work establishes a non-destructive and straight-forward statistical method to analyse the relationship between microbial distribution and metal alloy structure.